



Pergamon

SCIENCE @ DIRECT®

Bioorganic & Medicinal Chemistry 11 (2003) 2019–2023

BIOORGANIC &
MEDICINAL
CHEMISTRY

QSAR Study of Quinolinediones with Inhibitory Activity of Endothelium-Dependent Vasorelaxation by CoMSIA

Hea-Young Park Choo,^{a,*} Suyoung Choi,^a Chung-Kyu Ryu,^a Hwa-Jung Kim,^a
In Young Lee,^b Ae Nim Pae^b and Hun Yeong Koh^b

^a*School of Pharmacy, Ewha Womans University, Seoul 120-750, South Korea*

^b*Biochemicals Research Center, Korea Institute of Science and Technology, PO Box 131, Cheongryang, Seoul 130-650, South Korea*

Received 7 November 2002; accepted 8 January 2003

Abstract—The 3D-QSAR study of quinolinediones which showed potent inhibitory effect on the acetylcholine induced vasorelaxation of rat aorta with the endothelium was conducted by CoMSIA. The statistical result, cross-validated q^2 (0.741) and r^2 (0.960) values, gave reliability to the prediction of inhibitory activity of this series.

© 2003 Elsevier Science Ltd. All rights reserved.

Introduction

6-Anilino-5,8-quinolinedione (LY83583) has been widely used as an agent to reduce levels of nitric oxide (NO) dependent cGMP in tissues. This compound suppressed not only endothelium-dependent vasorelaxation, but also endothelium-independent relaxation induced by exogenous NO generated from nitrovasodilator drugs.^{1–3}

Quinones such as 1,4-naphthoquinones and 6-phenylamino-5,8-quinolindione showed the inhibition of the endothelium-dependent vasorelaxation.^{4–7} 6-Phenylamino-5,8-quinolindiones also produced the inhibition of L-arginine-induced vasorelaxation in endotoxin-treated rats, indicating their inhibitory effects on inducible NO synthase. 6-Phenylamino-5,8-quinolindiones lowered intracellular cGMP in several tissues due to inhibition of endothelial nitric oxide synthase activity and decreased in NO formation.³ Endogenous formation of NO from L-arginine is catalyzed by NO synthase. Isozymes of NO synthase consisting of neuronal, endothelial and inducible form have in common a NADPH-cytochrome P450 reductase domain. Quinonoids compounds undergo one- or two-electron reduction by flavoenzymes such as cytochrome P450 and shunts electrons away from L-arginin oxidation.⁴

The bioisosteres of these quinones, 6/7-(substituted-phenyl)amino-5,8-quinolinediones, 7-(substituted-phenyl)amino-5,8-isoquinolinediones and 6/7-(substituted-phenyl)amino-5,8-quinazolinediones were synthesized and their inhibitory activities on the ACh-induced vasorelaxation of PE-precontracted rat aorta with the intact endothelium were reported.^{8,9} In this series the presence of nitrogen on the heterocyclic quinones might be an important factor in the inhibitory activities. However, quantitative structure–activity relationship study for this series are not reported and here we report the QSAR of quinazolinediones on the inhibition of endothelium-dependent vasorelaxation.

Methods

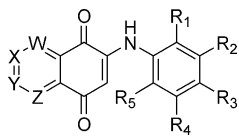
Data set for analysis

The inhibitory activities of endothelium-dependent vasorelaxation of 6/7-(substituted-phenyl)amino-5,8-quinolinediones, 7-(substituted-phenyl)amino-5,8-isoquinolinediones, 6/7-(substituted-phenyl)amino-5,8-quinazolinediones of Ryu were used for this analysis.^{8,9} Table 1 represents the structure and endothelium-dependent vasorelaxation inhibition activities (EC₅₀, µg/mL) of compounds employed in this study.

Computational methods

All molecular modeling and statistical analyses were performed using SYBYL 6.5 molecular modeling

*Corresponding author. Tel.: +82-2-3277-3042; fax: +82-2-3277-2851; e-mail: hypark@mm.ewha.ac.kr

Table 1. Structure of quinolinedione derivatives


Compd	W	X	Y	Z	R ₁	R ₂	R ₃	R ₄	R ₅	EC ₅₀ (μM)
1 ^a	C	N	C	N	H	H	F	H	H	0.846
2	C	N	C	N	H	H	Br	H	H	0.534
3	C	N	C	N	H	I	H	H	H	0.664
4	C	C	C	N	H	H	F	H	H	0.541
5	C	C	C	N	H	H	Br	H	H	0.302
6	C	C	C	N	H	H	I	H	H	0.214
7	C	C	C	N	H	H	CF ₃	H	H	0.607
8	C	N	C	C	H	F	F	H	H	0.640
9	C	N	C	C	H	F	H	F	H	0.290
10	C	N	C	C	F	H	F	H	H	0.430
11	C	C	C	C	H	H	H	H	H	0.239
12	C	C	C	C	H	H	F	H	H	0.362
13	C	C	C	C	F	F	F	H	H	0.330
14	N	C	N	C	H	H	Br	H	H	0.599
15	N	C	N	C	H	H	F	H	F	0.708
16	N	C	N	C	H	H	H	H	F	0.624
17	N	C	N	C	H	F	H	F	H	0.475
18	N	C	N	C	H	H	CH ₃	H	H	0.503
19	N	C	N	C	H	H	CF ₃	H	H	0.599
20	N	C	N	C	H	H	OCF ₃	H	H	0.615
T1 ^b	C	N	C	N	H	H	Cl	H	H	1.036
T2	C	N	C	N	H	F	H	H	H	0.437
T3	C	N	C	N	H	H	CF ₃	H	H	1.269
T4	C	C	C	N	H	F	H	F	H	0.449
T5	C	C	C	N	H	H	OCF ₃	H	H	0.603
T6	C	N	C	C	H	H	H	H	H	0.439
T7	C	N	C	C	H	F	H	H	H	0.562
T8	C	C	C	C	H	H	Cl	H	H	0.220
T9	N	C	N	C	H	H	H	H	H	0.340
T10	N	C	N	C	H	H	Cl	H	H	0.861
T11	N	C	N	C	H	H	F	F	F	0.919

^a1–20: Training set.^bTest set.

software (Tripos Inc.) and Silicon Graphics Indy workstation (IRIX 6.2). The 2D structure of each compound was built using SYBYL Build program with the default SYBYL settings. The 2D structure was converted to a 3D structure using Concord 4.0 program. The structural energy minimization was performed using the SYBYL energy minimizer (Tripos Force Field) and Gasteiger–Huckel charge or AM1 semiempirical quantum mechanical charge, with a 0.005 kcal/mol energy gradient convergence criterion. Low energy conformation was searched by geometry optimization after rotating every 30° of single bond from 1 to 330° of torsional angle. All of the structures generated were aligned into lattice box by fitting with 2-aryl amino quinone group as a common structure.

Calculation of CoMSIA descriptors

The CoMSIA of the QSAR module of SYBYL was used for the analysis. Similarity indices between a compound and a probe atom were calculated. The common probe atom with charge +1, radius 1 Å, and hydrophobicity +1 was placed at the intersections of a regularly spaced lattice. The attenuation factor (α) was set

at 0.3. To determine the similarity, the mutual distance between probe atom and the atoms of the molecules in the data set was considered. In this study physicochemical properties such as steric and electrostatic feature, hydrogen bond donors and acceptors, and hydrophobic fields were considered.

The equation used to calculate the similarity indices is as follows.

$$A_{F,K,(j)}^q = -\sum W_{\text{probe},k} W_{ik} e^{-\alpha r_{iq}^2}$$

A is the similarity index at grid point q , summed over all atoms i of the molecule j under investigation. $W_{\text{probe},k}$ is the probe atom with radius 1 Å charge +1, hydrophobicity +1, hydrogen bond donating +1, and hydrogen bond accepting +1. W_{ik} is the actual value of the physicochemical property k of atom i . The mutual distance between the probe atom at grid point q and atom i of the test molecule is represented by r_{iq} . α is the attenuation factor, with a default value of 0.3, and an optimal value normally between 0.2 and 0.4, larger values of which result in a steeper Gaussian function curves and a strong attenuation of the distance-dependent effects of molecular similarity.

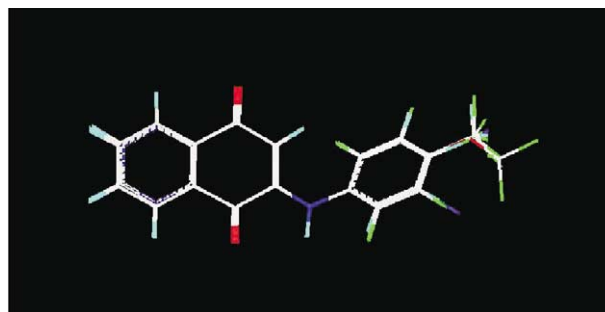
The partial least squares (PLS) method was used for fitting the 3D structural features and their biological activities. The optimum number of components in the final PLS model was determined by the q^2 value, obtained from the leave-one-out cross validation technique.

Molecular alignment

Using compound 6 as template molecule, superposition of all quinolinediones was performed with common 2-phenylamino quinone containing in all compounds. Figure 1 shows the results of such alignment.

Results and Discussion

Firstly, CoMFA, the most commonly used QSAR program, was employed for the analysis with the training set composed of 20 various analogues, which biological activities are known. All three models showed low correlation (q^2 values: 0.405–0.563) and overstated ONC values (8–10) with steric, electrostatic fields,

**Figure 1.** Stereoview of the 20 compounds aligned.

lipophilicity, and/or CMR as shown in Table 2. Probably the data set in which the structure of compounds analysed were so similar and the activities were in narrow range might cause the poor result.

In CoMFA model I, the relative contributions of electrostatic and steric field were 59.7 and 40.3%, respectively. In the second model, electrostatic and steric field were 42.7 and 36.6%, respectively, and that of ClogP was 20.7%. The contributions of CMR was negligible in model III.

QSAR analysis using CoMSIA with the same data set was accomplished. Two charges (Gasteiger–Huckel and AM1) and two optimized structures using MM and AM1 method were considered in the QSAR study. Thus, a total of four models were constructed.

Statistical results of the CoMSIA are summarized in Table 3. CoMSIA with AM1 charge were used as descriptors, and the inhibition of vasorelaxation activities of rat aorta as a dependent column.

A cross-validated value q^2 which was obtained as a result of PLS analysis served as a quantitative measure of the predictability of the CoMSIA model. From Table

3, we found that the result was less sensitive to charge evaluation methods but the models minimized using tripos force field showed higher q^2 values than those for AM1 optimized sets.

Among the four models tested, the best predictive power was the second model judging from higher cross-validated and non-cross-validated correlation and proper ONC value (Table 3). Good cross-validated q^2 (0.741) and conventional r^2 (0.960) values proved the correlation between the descriptors and each of their activities. The relative contributions of electrostatic field and lipophilicity were 43.4 and 26.4%, respectively, and that of hydrogen bond acceptor field was 26.5%. Hydrogen bond acceptor/donor could not be considered in CoMFA analysis and the additional fields might improve the results of CoMSIA model. The contributions of steric fields and hydrogen bond donor field were negligible. The measured and estimated activities of the training set are reported in Table 4. Figure 2 shows good linear correlation (slope = 0.979, intercept = 0.003, regression = 0.997, $n = 20$) and small difference between estimated and measured values (average value of residuals = 0.03).

The best way to validate a CoMSIA model is to predict theoretical values for some compounds whose experimental values are known but not included in the training set (called test set). Eleven molecules chosen for testing were T1–T11 shown in Table 1. Each of these structures was built up by starting from the most similar molecule in the training set and performing necessary structural changes. New structures were also minimized using the same method applied to the compounds in the training set.

The CoMSIA analysis of the test set composed of 11 compounds was reported in Table 5. Most of the com-

Table 2. QSAR results by using CoMFA

	Model I CoMFA(SF/EF)	Model II CoMFA/ClogP	Model III CoMFA/ClogP/CMR
ONC ^a	10	8	9
q^2 ^b	0.563	0.551	0.405
r^2 ^c	0.990	0.983	0.984
SEE ^d	0.025	0.029	0.029
F ^e	86.713	77.401	68.928
SF	40.3%	36.6%	35.9%
EF	59.7%	42.7%	43.3%
ClogP		20.7%	19.7%
CMR			1.0%

^aOptimum number of component.

^bCross validated r^2 .

^cNon-cross validated r^2 .

^dStandard error estimate.

^eFraction of explained versus unexplained variance.

Table 3. QSAR results by using CoMSIA

Method	MM		AM1 (optimization)	
	1. Gasteiger–Huckel	2. AM1	3. Gasteiger–Huckel	4. AM1
ONC	7	5	7	5
q^2	0.667	0.741	0.532	0.591
r^2	0.964	0.960	0.960	0.915
SEE	0.040	0.039	0.042	0.057
F	46.300	67.563	41.207	30.233
SF ^a	3.6%	3.6%	4.9%	3.9%
EF ^b	44.4%	43.4%	43.2%	41.2%
LF ^c	28.3%	26.4%	28.5%	27.4%
HDF ^d	0.1%	0.2%	1.2%	1.6%
HAF ^e	23.5%	26.5%	22.3%	26.0%

^aSteric field contribution.

^bElectrostatic field contribution.

^cLipophilic field.

^dHydrogen bonding donor field.

^eHydrogen bond acceptor field.

Table 4. Measured and estimated activities of 20 compounds in the training set

Compd	Measured ^a	Estimated ^b	Residual ^c
1	0.07	0.06	0.01
2	0.28	0.30	0.03
3	0.18	0.17	0.01
4	0.27	0.25	0.01
5	0.52	0.49	0.03
6	0.68	0.67	0.00
7	0.21	0.26	0.05
8	0.19	0.26	0.06
9	0.54	0.50	0.04
10	0.37	0.33	0.04
11	0.62	0.62	0.00
12	0.44	0.46	0.02
13	0.48	0.47	0.01
14	0.41	0.40	0.01
15	0.15	0.11	0.04
16	0.21	0.26	0.05
17	0.33	0.37	0.04
18	0.30	0.32	0.02
19	0.22	0.18	0.04
20	0.21	0.17	0.03

^aExperimentally measured activity values (log 1/EC₅₀).

^bTheoretically estimated activity values (log 1/EC₅₀).

^cMeasured–Estimated.

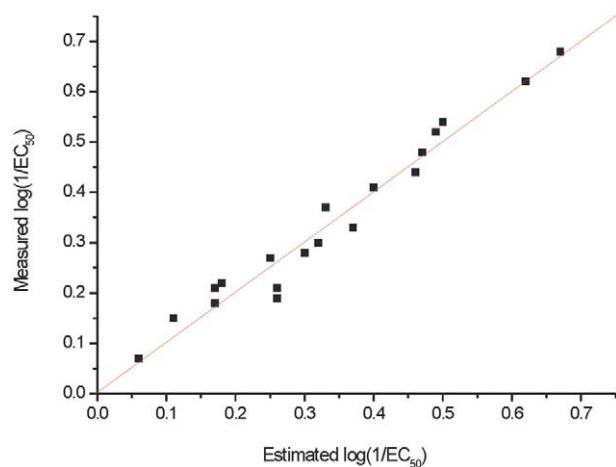


Figure 2. Measured versus estimated inhibitory activities of vaso-relaxation in the training set.

Table 5. Measured and estimated activities of 11 compounds in the test set

Compd	Measured ^a	Estimated ^b	Residual ^c
T1	−0.02	0.15	0.17
T2	0.35	0.18	0.17
T3	−0.10	0.08	0.18
T4	0.35	0.46	0.12
T5	0.22	0.26	0.04
T6	0.36	0.44	0.09
T7	0.25	0.41	0.16
T8	0.66	0.54	0.11
T9	0.47	0.32	0.15
T10	0.06	0.24	0.18
T11	0.04	0.20	0.17

^aExperimentally measured activity values (log 1/EC₅₀).

^bTheoretically estimated activity values (log 1/EC₅₀).

^cMeasured–Estimated.

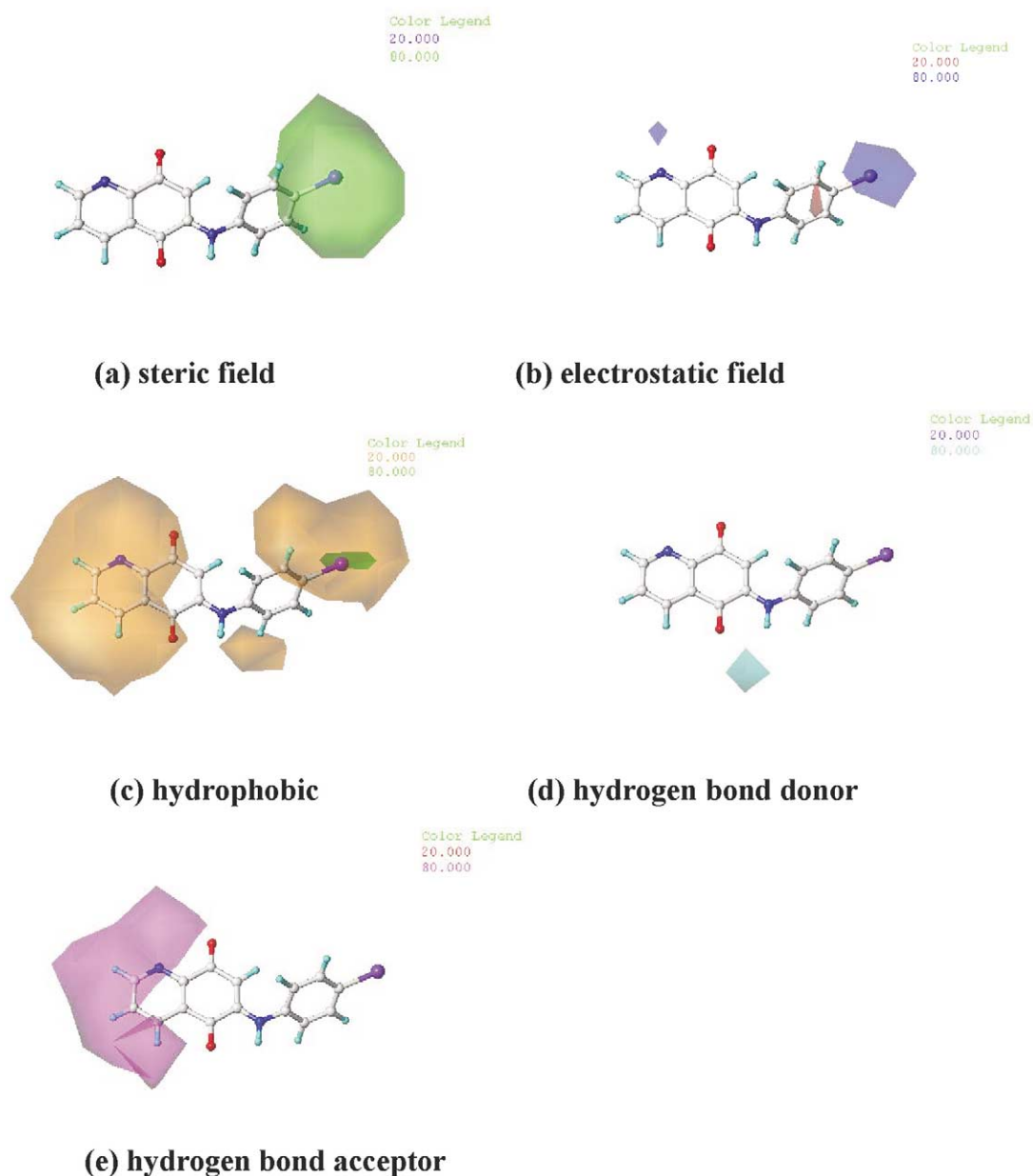


Figure 3. CoMSIA contour map.

pounds tested showed good agreement between actual and predicted values. The mean deviation between experimental and predicted binding affinity is 0.14 log unit and gave reliability to the prediction of the activities of the test set.

The contour maps derived from the best model was used to display the contributions of five fields of CoMSIA map, steric/electrostatic/lipophilic/hydrogen bond donor/hydrogen bond acceptor ability (Fig. 3). The contour plots give a direct visual indication of which parts of the molecules differentiate the activities of the compounds in the set under study. The plots also offer an interpretation as to how to design new molecules which can show much higher binding affinity.

Each contour map is colored in two different colors for positive and negative effects. In other words, the steric features are green (more bulk increases bioactivity) and purple (bulkier substituents decrease bioactivity), and the electrostatic features are red (more negative charge increases bioactivity) and blue (the same but for positive charge). Then, lipophilic features are green (favored) and orange (disfavored), and hydrogen bond donor features are also cyanide (favored) and purple (disfavored), and finally, hydrogen bond acceptor features are magenta (favored) and red (disfavored), respectively.

CoMSIA was successful in the correlation of the structural features of the quinolinediones analogues with their binding affinity. The values of the CoMSIA q^2 (0.741) and r^2 (0.960) indicate satisfactory agreement between observed and predicted $\log(1/EC_{50})$ values.

Three features (electrostatic/lipophilic/hydrogen bond donor ability) made great contribution to specific interaction of these analogs with the receptor. The electrostatic contour map exhibited a major favorable region, which is coded in blue color. That region was located in the *para* position of amino group and iodo substituent in the highest activity compound **6** was well mapped to that position.

Lipophilically unfavorable region, which was coded in orange color, was located through a large scope. It is represented that the hydrophilicity is the major driving force in these compounds and has something in common with the large contribution of the above electrostatic field.

3D-QSAR analysis result indicates the introduction of electron withdrawing group or hydrophilic group on phenyl group enhances inhibitory activity in this series of compounds. However, the location of nitrogens in the quinazoline ring was not important for the activity. This analysis may provide useful information in the design of new inhibitor. The inhibitor of endothelium-dependent vasorelaxation would be useful for the treatment of sepsis, circulatory shock, stroke and inflammation.

Conclusions

3D-QSAR studies of quinolinediones which showed potent inhibitory effect on the acetylcholine induced vasorelaxation of rat aorta with the endothelium were conducted using CoMFA and CoMSIA method. CoMFA models only considered of electrostatic, steric factor and lipophilicity for the correlation. By comparing these two methods applied to this set, the CoMSIA model provided significant correlation and predictive power.

Acknowledgements

This work was supported by a grant from Korea Research Foundation (M10022040004-01G0509-00710-07).

References and Notes

1. Muelsch, A.; Busse, R.; Loeb, S.; Fostermann, U. *J. Pharmacol. Exp. Ther.* **1988**, *247*, 283.
2. Luo, D.; Das, S.; Vincent, S. R. *Eur. J. Pharmacol.* **1995**, *290*, 247.
3. Kumagai, Y.; Midorikawa, K.; Nakai, Y.; Yosikawa, T.; Kushida, K.; Homma-Takeda, S.; Shimojo, N. *Eur. J. Pharmacol.* **1998**, *360*, 213.
4. Kumagai, Y.; Nakajima, H.; Midorikawa, K.; Homma-Takeda, S.; Shimojo, N. *Chem. Res. Toxicol.* **1998**, *6*, 608.
5. Lee, J.; Lee, M. Y.; Chung, S. M.; Chung, J. H. *Toxicol. Appl. Pharmacol.* **1999**, *161*, 140.
6. Ryu, C. K.; Jung, S. H.; Lee, J. A.; Kim, H. J.; Lee, S. H.; Chung, J. H. *Bioorg. Med. Chem. Lett.* **1999**, *9*, 2469.
7. Lee, J. A.; Jung, S. H.; Bae, M. K.; Ryu, C. K.; Lee, J. Y.; Chung, J. H.; Kim, H. J. *Gen. Pharmacol.* **2000**, *34*, 33.
8. Ryu, C. K.; Shin, K. H.; Seo, J. H.; Kim, H. S. *Med. Chem. Res.* **2001**, *10*, 605.
9. Ryu, C. K.; Shin, K. H.; Seo, J. H.; Kim, H. S. *Eur. J. Med. Chem.* **2002**, *37*, 77.